

**Supplementary Information for:**

**Neural coding during active somatosensation revealed using illusory touch**

Daniel H. O'Connor<sup>1,\*,†</sup>, S. Andrew Hires<sup>1,\*</sup>, Zengcai V. Guo<sup>1</sup>, Nuo Li, Jianing Yu, Qian-Quan Sun<sup>1,#</sup>, Daniel Huber<sup>1,%</sup>, Karel Svoboda<sup>1</sup>

<sup>1</sup> Janelia Farm Research Campus, HHMI, Ashburn VA 20147

<sup>†</sup> Current address: The Solomon H. Snyder Department of Neuroscience & Brain Science Institute, The Johns Hopkins University School of Medicine, Baltimore, MD 21205

<sup>#</sup> Current address: Department of Zoology and Physiology, University of Wyoming, Laramie, Wyoming 82071

<sup>%</sup> Current address: Department of Basic Neurosciences, University of Geneva, CH-1211 Geneva, Switzerland.

\* These authors contributed equally to this work.

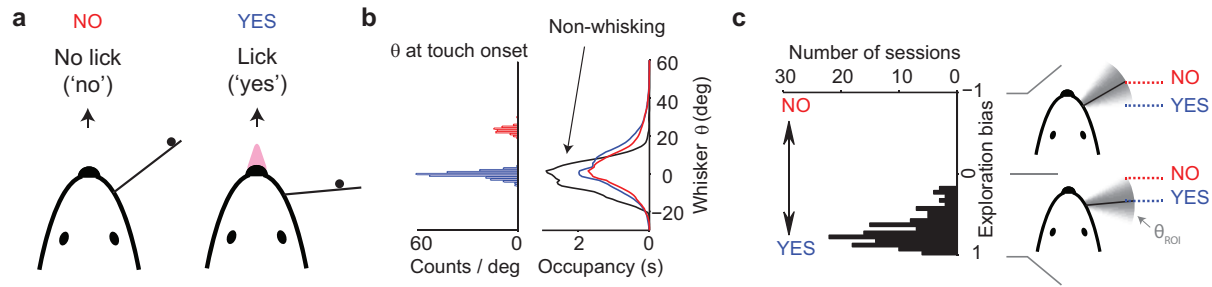


**Figure 1 | Whisking strategy underlying the object location discrimination task.**

- Schematic of the basic object location discrimination task. On NO trials the object was further away from the resting position of the whisker and required withholding a lick response (i.e., a ‘no’ response). On YES trials the object was closer and required a lick response (a ‘yes’ response).
- Whisking during object location discrimination. Left, whisker  $\theta$  at touch onset (295 touches; YES trials, blue; NO trials, red; one example session, different from Fig. 1c). Right, distribution of whisker positions during non-whisking (black; whisking amplitude,  $\theta_{\text{amp}} < 2.5$  degrees; Methods) and whisking periods ( $\theta_{\text{amp}} > 2.5$  degrees). Occupancy (in seconds) is the time spent at a particular  $\theta$  (bin size, one degree).
- Exploration bias for 148 behavioral sessions. This measures the preference of the  $\theta_{\text{ROI}}$  for one pole position compared to the other. The two pole positions were defined as the distribution of  $\theta$  at touch onset for all exploration period touches, normalized to 1. These pole position distributions were multiplied by the whisker occupancy during active whisking. These two products ( $p_1$ ,  $p_2$ ) were combined  $(p_1 - p_2) / (p_1 + p_2)$  to generate the exploration bias for the behavioral session. Mice preferentially explored one pole location (exploration bias  $\neq 0$ ). Exploration bias less than 0 indicates a tendency to explore the NO location. Exploration bias greater than 0 indicates a tendency to explore the YES location.

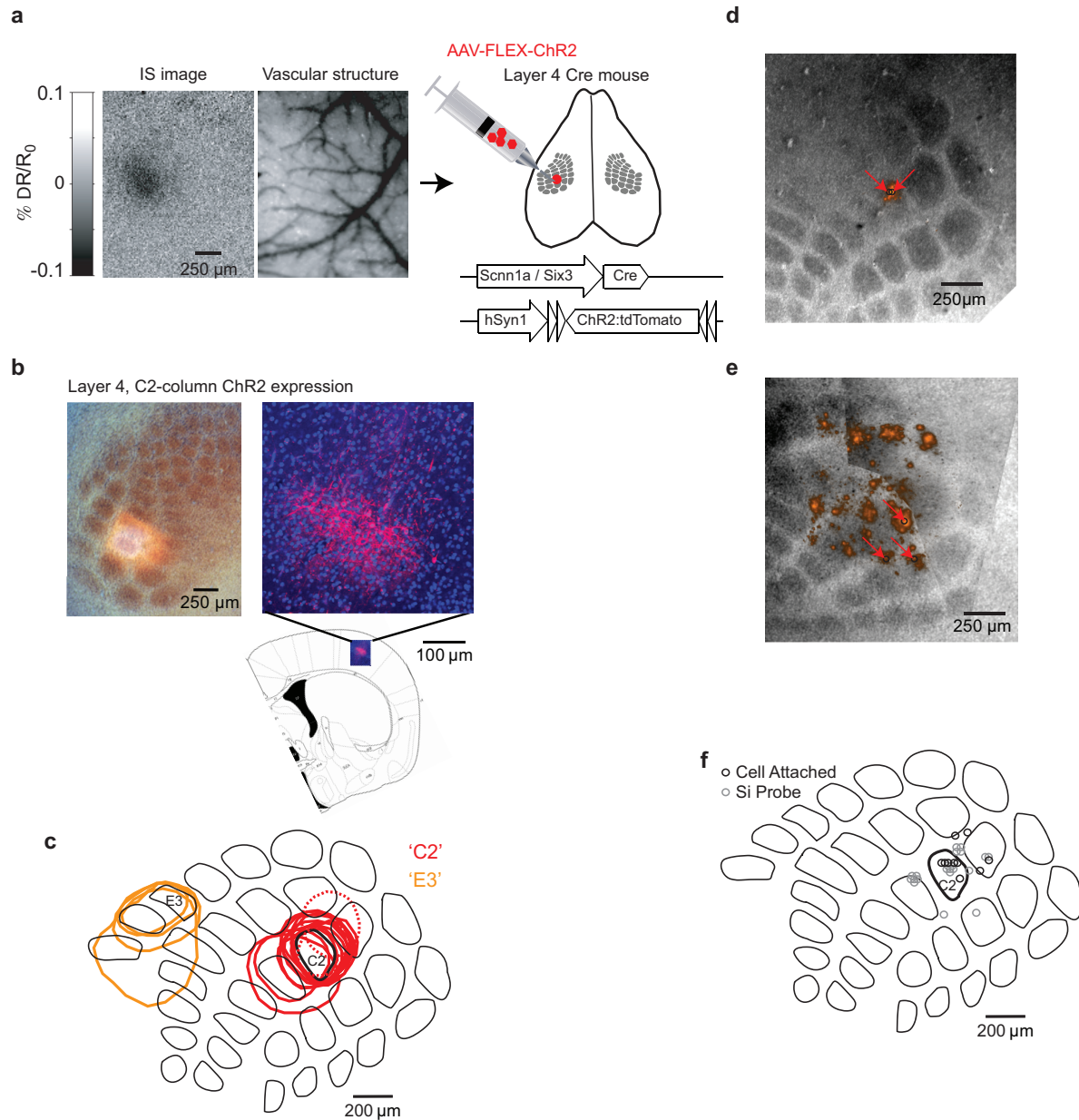


**Figure 2 | Targeting layer 4 of the C2 barrel column for ChR2 expression and recording.**

- Viral gene delivery targeted by intrinsic signal imaging. Intrinsic signal image (left) taken through the intact skull and used to localize the C2 (or E3) barrel column next to an image of the vascular landmarks (middle). Subsequent to intrinsic signal imaging-based mapping, Cre-dependent virus is injected into the relevant barrel in L4 Cre mice (right).
- Analysis of ChR2 expression. Left, flattened and cytochrome oxidase-stained section through barrel cortex, showing ChR2-tdTomato fluorescence in the C2 barrel column. Right, a coronal section showing ChR2-tdTomato fluorescence (magenta) and nuclei (DAPI, in blue).

- c. Labeling accuracy for AAV injections targeted to C2 (red) or E3 (yellow). The contour lines encompass the labeled somata. Dotted lines show the best estimate for the two cases in which there was some ambiguity about barrel identity due to imperfect histology. The barrel map schematic is based on data from <sup>55</sup>.
- d. Reconstructing recording locations. Flattened and cytochrome oxidase-stained section through barrel cortex, overlaid with DiI fluorescence introduced by a cell-attached recording electrode. Estimated L4 cell locations (2) marked with red arrows.
- e. Composite of two flattened and cytochrome oxidase-stained sections through barrel cortex with DiI overlay from silicon probe recording. Estimated neuronal locations (3) are marked with red arrows.
- f. Location of recordings during object location discrimination behavior (**Figs. 1, 2**).

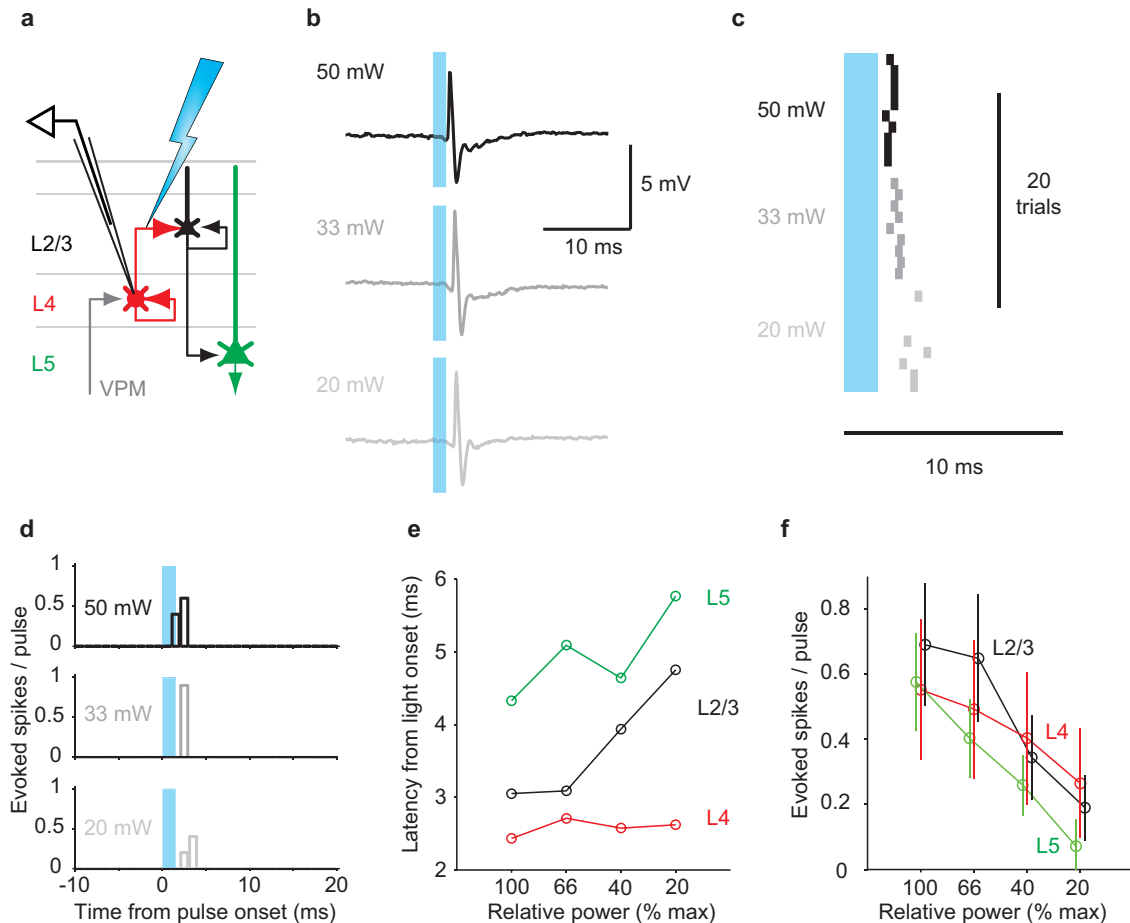


**Figure 3 | Calibration of ChR2-based photostimulation.**

- Schematic of the recording configuration. Loose cell-attached recordings were made from neurons in all cortical layers ( $n=85$  neurons total;  $N=10$  mice). L6 neurons did not produce evoked spikes in response to photostimulation (cf. **Fig. 4c**) and they are not shown. Responses to photostimulation of L4 neurons were measured.
- Example action potential responses from a single L4 neuron to short pulses of blue light at different power levels (50, 33, and 20 mW).
- Spike raster showing trials from the neuron in b.
- Peristimulus time histogram for the neuron shown in b.
- Latency of evoked spikes as function of power, across cortical layers. Plot symbols show the mean across neurons. Because of the trade-off between maximum intensity and pulse duration, to pool neurons we occasionally report “Relative power” as a percentage of the maximum power (see Methods).
- Number of evoked spikes as function of power, across cortical layers. Plot symbols show the mean across neurons. Error bars show bootstrap SEM across neurons. L2/3 activity

appears less sparse than expected based on previous *in vivo* imaging and electrophysiology experiments<sup>12</sup>. It is possible that differences in the recruitment of feedforward inhibition between photostimulation and natural touch may underlie the differential recruitment of L2/3 neurons. For example, cross-whisker inhibition is expected in multi-whisker behavior<sup>12</sup> and may promote sparseness in L2/3 responses. It is also possible that the somewhat more synchronous excitation of L4 by photostimulation vs. natural touch (**Fig. 4**) may drive more efficient excitation of L2/3 neurons.

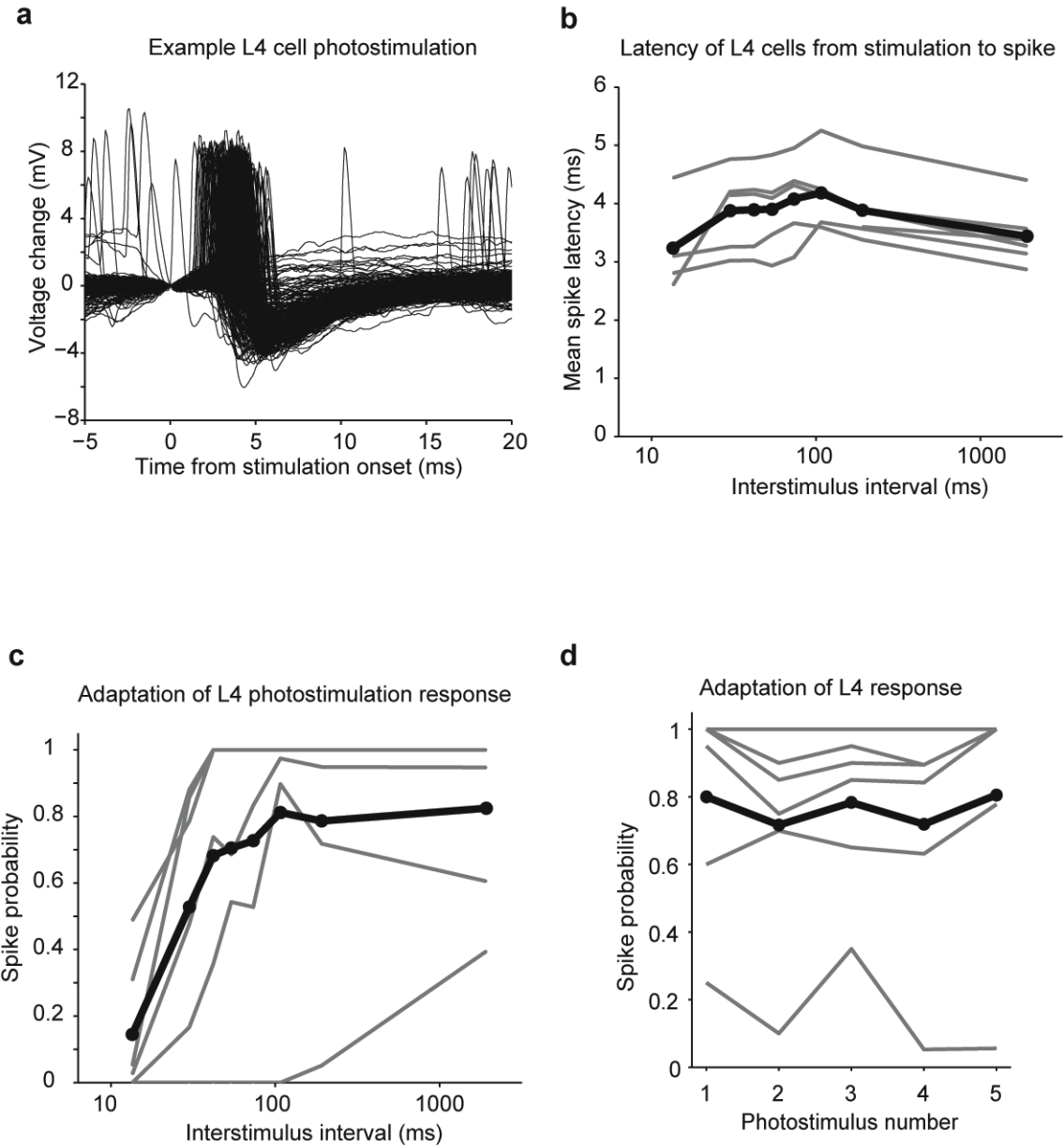
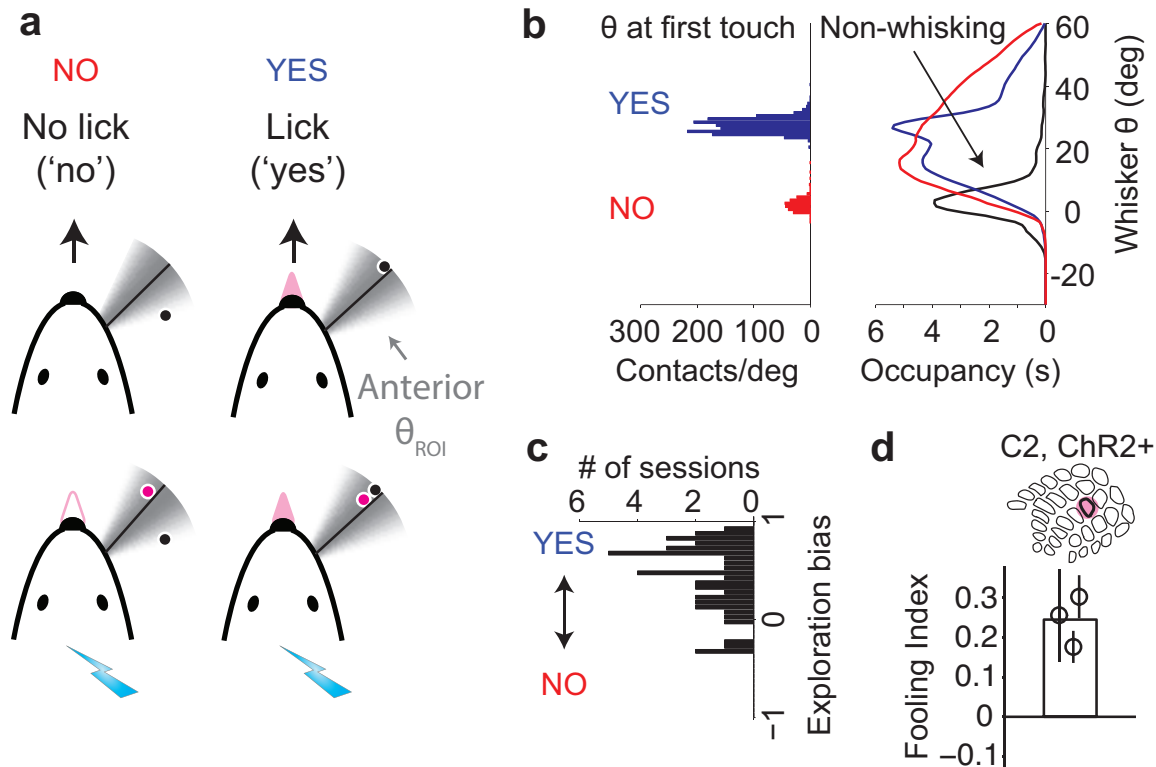


**Figure 4 | Reliability of L4 ChR2-positive neuron responses during naturalistic photostimulation.**

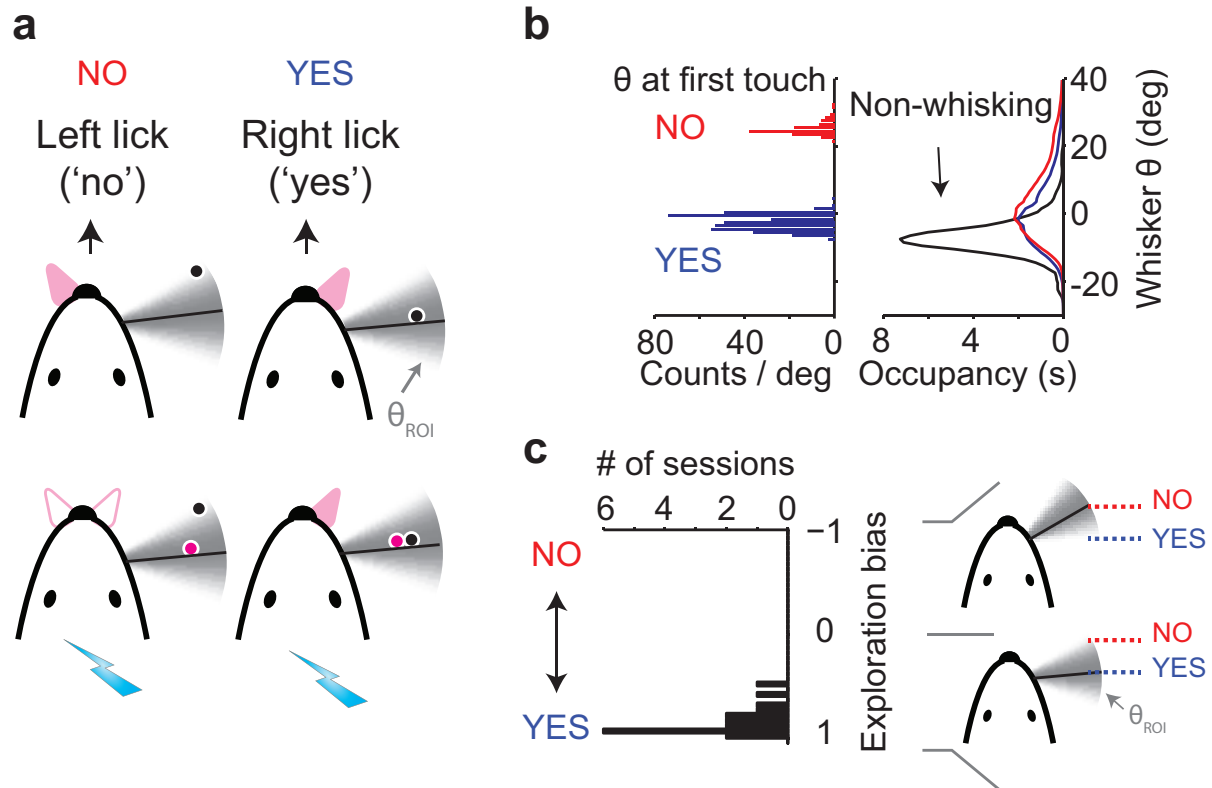
- Extracellular voltage traces from an L4 neuron via loose-seal cell attached recording during naturalistic photostimulation. Photostimulation trains were chosen from a set of whisker crossings obtained from the object location discrimination task (in which mice determined the pulse train pattern by their whisking; Methods).
- Evoked spike latency as a function of interstimulus interval for individual cells (grey) and the population mean (black,  $n=6$  cells).
- The probability of photostimulation evoking a spike as a function of interstimulus interval. Color conventions as in panel b.

- d. The probability of photostimulation evoking a spike as a function of the sequential photostimulus number within a train (first, second, etc). Color conventions as in panel b.



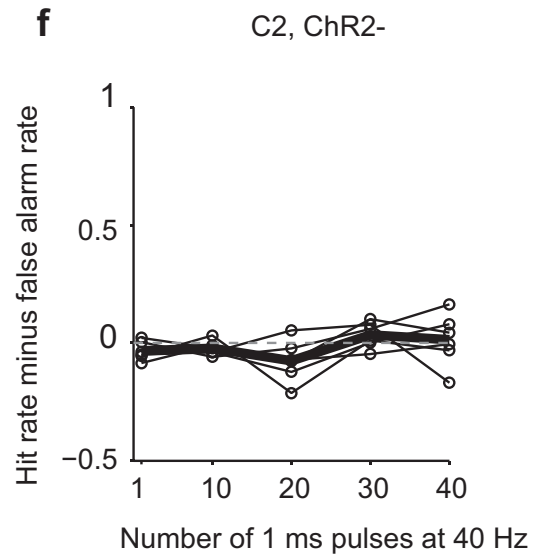
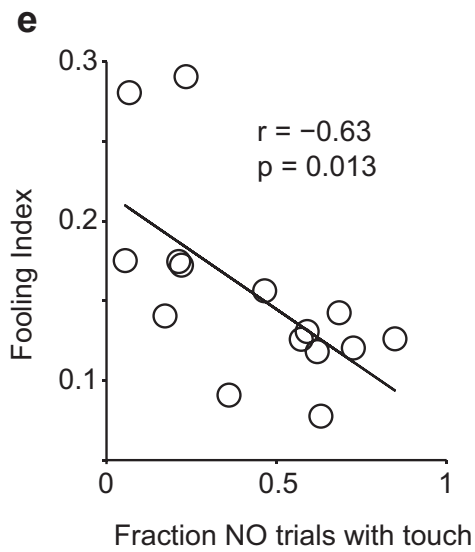
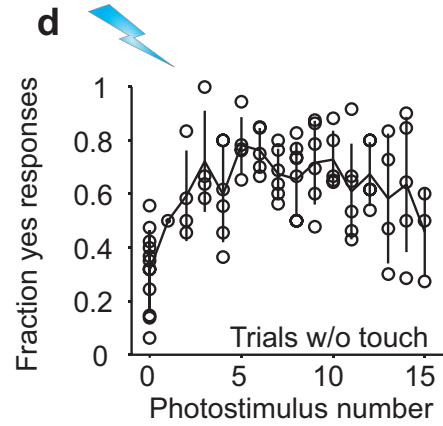
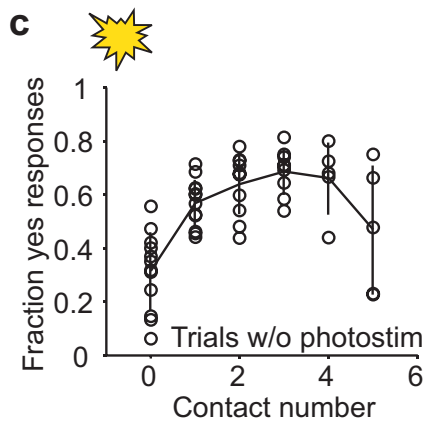
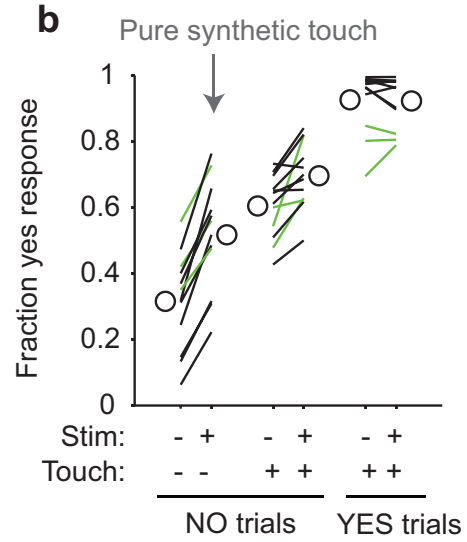
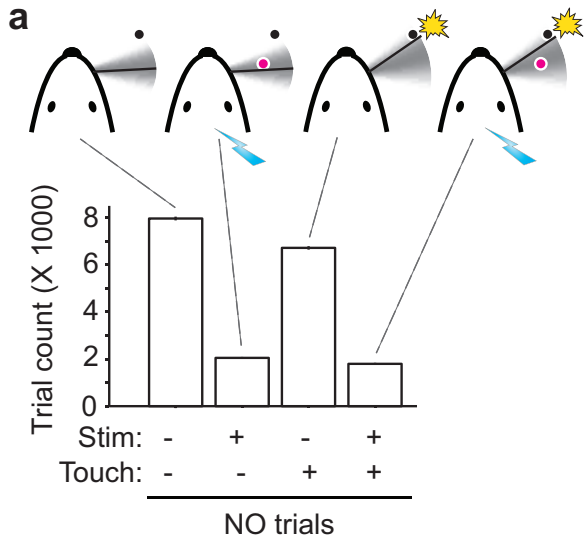
**sFigure 5 | Illusory touch occurs robustly when the YES location is anterior and the NO location is posterior.**

- Schematic of the experiment and the four trial types. As in **Fig. 5**, except that the YES and NO locations were switched with respect to the experiments of **Fig. 5**. Correspondingly, the  $\theta_{ROI}$  was anterior, as mice chose to focus whisking on the rewarded location, even though it was further from the resting position of the whisker.
- Quantification of whisker occupancy and contact probability, as in **Fig. 1**, **sFig. 1b**. . Left, whisker  $\theta$  at touch onset (1,490 touches). Black line shows whisker occupancy when the mouse is not whisking (i.e. the 'resting position' of the whisker). Occupancy (in seconds) is the time spent at a particular  $\theta$  (bin size, one degree).
- Quantification of whisking exploration bias, as in **sFig. 1c**.
- Photostimulation increases the fraction of yes responses in NO trials. Error bars, SEM.



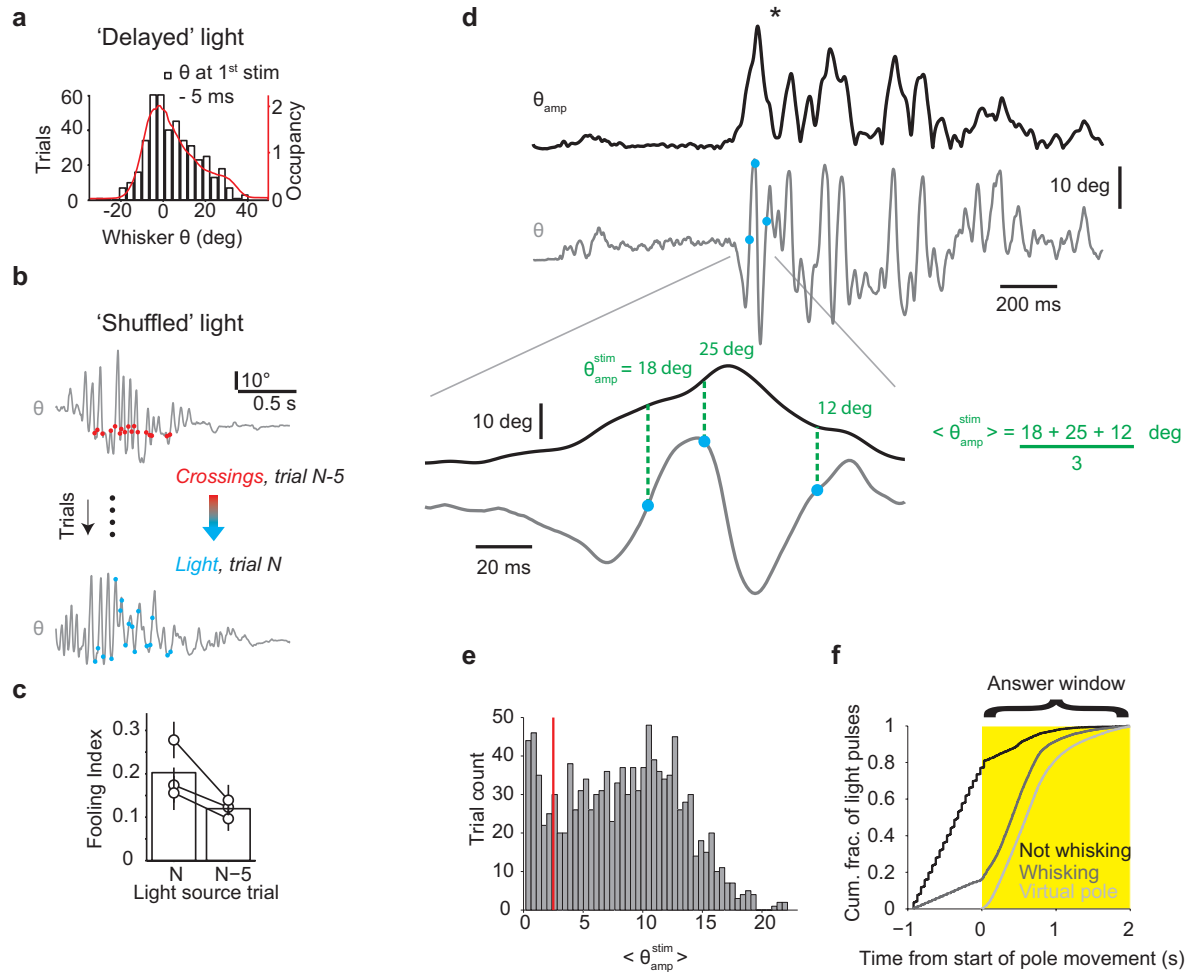
**sFigure 6 | Whisking strategy in the symmetric response task is the same as in the go/no-go task.**

- Symmetric response task; both object locations were indicated by licking at one of two lickports (lick left / lick right).
- Whisking strategy in the symmetric response task. Same units as **Fig. 1c**.
- Exploration bias for 18 symmetric response sessions (see Methods). Mice preferentially explored one pole location (exploration bias  $\neq 0$ ).



## sFigure 7 | Interactions between illusory and real touch.

- a. We examined interactions between activity evoked by photostimulation and touch, capitalizing on trial-to-trial variability in behavior and the large numbers of trials in our experiments (mean, 3007 trials over 9 sessions per mouse). We sorted behavioral trials into four groups based on the presence of touch contact (yellow explosion) and/or photostimulation (blue bolt). The histogram shows the number of trials of each type, for NO trials.
- b. Fraction of yes responses depending on touch and photostimulation. Each line corresponds to one mouse. Black lines, lick / no lick task; green lines, symmetric response task. Real touch on NO trials increased ‘yes’ responses ( $p < 0.001$ , paired one-tailed t-test). In trials without contact, photostimulation also drove ‘yes’ responses ( $p < 0.001$ ), to levels comparable to NO trials with contact ( $p = 0.099$ ). However, in NO trials with contact, photostimulation had less additional effect ( $p = 0.002$ , paired one-tailed t-test on difference in photostimulation effect). These data indicate that photostimulation and touch occlude each other, and thus provide evidence that real touch and illusory touch are perceptually similar.
- c. Rapid saturation of perception-driven choice with the number of stimuli (contacts or photostimuli) might underlie the occlusion shown in panel b. On trials without photostimulation, the fraction of ‘yes’ responses on NO trials showed a large increase with the first contact, but only small additional increases thereafter. Fraction of yes responses therefore saturates rapidly with the number of touches. Error bars, STD.
- d. On trials without touch, photostimulation-driven ‘yes’ responses showed equally rapid saturation (compared with touch-driven ‘yes’ responses shown in panel c). Error bars, STD.
- e. Across-animal analysis of the Fooling Index vs. the fraction of NO trials with touch during the exploration window. Animals that touched more often were less fooled, due to occlusion of fooling by touch.
- f. Detection of light pulse trains over the C2 column is difficult or impossible for a sham infected (ChR2<sup>-</sup>) mouse. Light detection (75 mW) psychometric-style curve for a highly trained ChR2-negative mouse. Thin lines show individual sessions, thick lines show the mean. Mouse was a Tg(Etv1-cre)GM225Gsat mouse with a ‘sham’ AAV injection; virus was injected in the C2 column but the mouse was confirmed ChR2-negative, for unknown reasons, by histology.



**sFigure 8 | Illusory touch does not require precisely timed or sequenced spikes, but only occurs only during whisking**

- Distribution of  $\theta$  at first stimulus for delayed light trials (**Fig. 6**) with  $\Delta t \geq 20$  ms ( $-5$  ms, to correct for the difference in the delay between photostimulus and spike versus touch and spike; cf. **Fig. 4**). Red line, whisker occupancy.
- We next determined if the precise sequence of inter-photostimulation intervals mattered for illusory touch. We interleaved the standard experiment ( $\Delta t = 5$  ms) with trials in which a photostimulus pattern corresponded to a whisking pattern measured in a previous trial ( $N-5$ , where  $N$  is the current trial; 'shuffled' light). Under these conditions the statistical features of the photostimulus pattern are matched across the different types of stimulated trials, but the patterns of whisker crossings does not predict the pattern of photostimuli within a trial.
- On the shuffled photostimulation trials mice were still fooled, although the effect was smaller than for the standard experiment (Fooling Index 0.12 vs. 0.20; 1 of 3 mice  $p <$

0.05, two-tailed permutation test). These experiments show that illusory touch does not require L4 activity to match the precise pattern of virtual pole crossings.

- d. Schematic showing the measurement of mean  $\theta_{amp}$  at the time of stimulation. Blue circles indicate light pulse times. Asterisk indicates response lick time.
- e. Mean  $\theta_{amp}$  at the time of stimulation. Red line shows the criterion ( $\theta_{amp}; 2.5$  deg) used to separate trials into 'whisking' and 'not whisking'.
- f. Distribution of light pulses across times within the trial, for trials with different categorizations. 'Virtual pole' trials refer to the standard  $\Delta t = 5$  ms trials. 'Answer window' is the time in which licks were scored as responses.

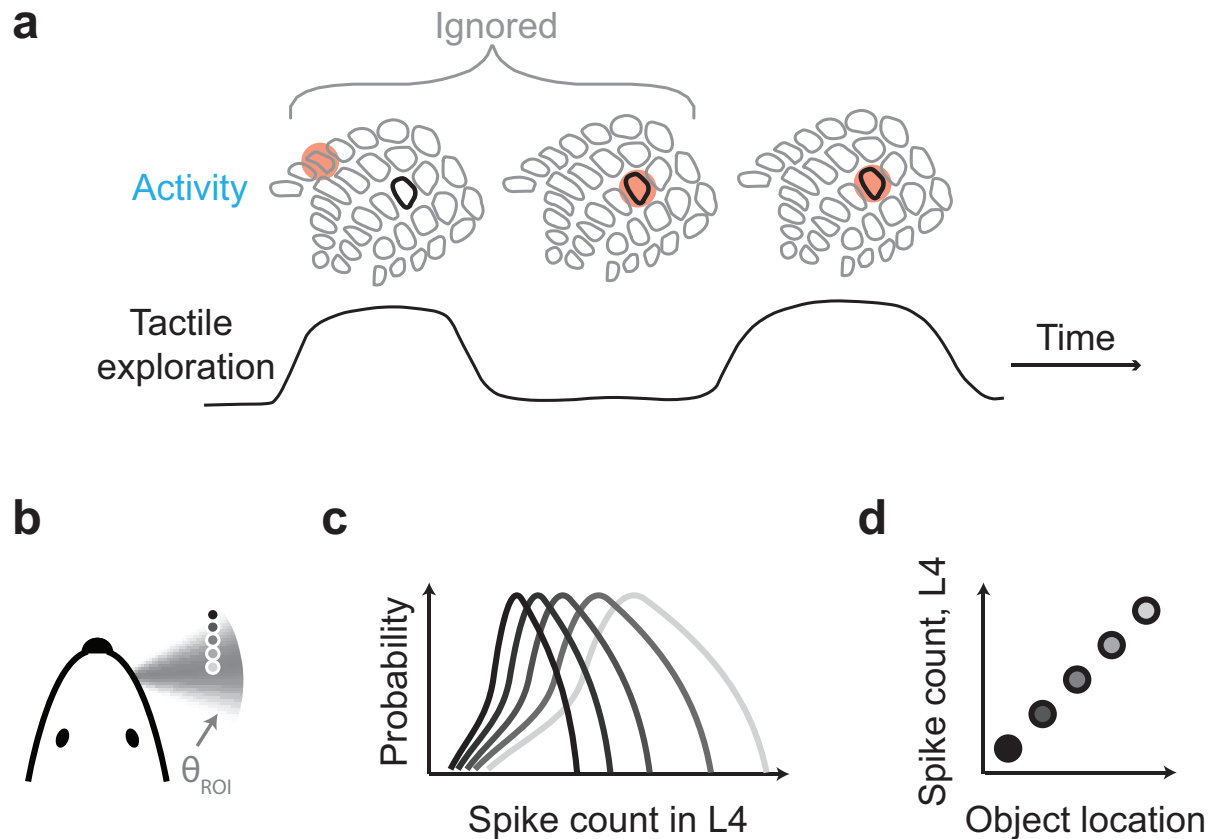
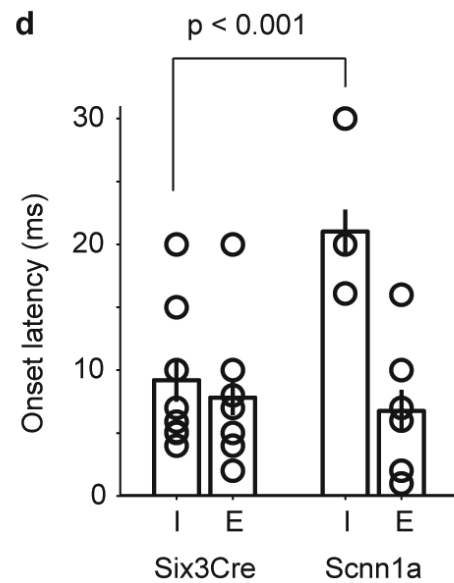
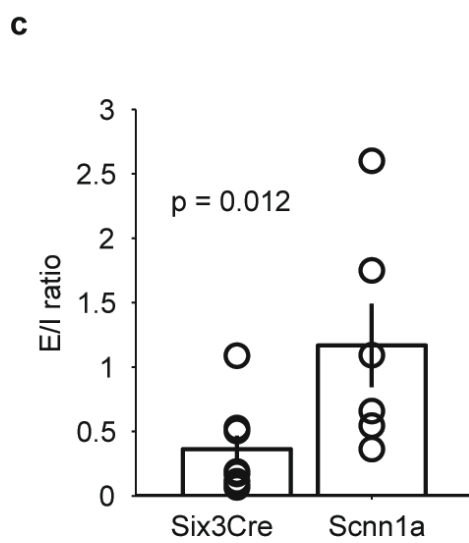
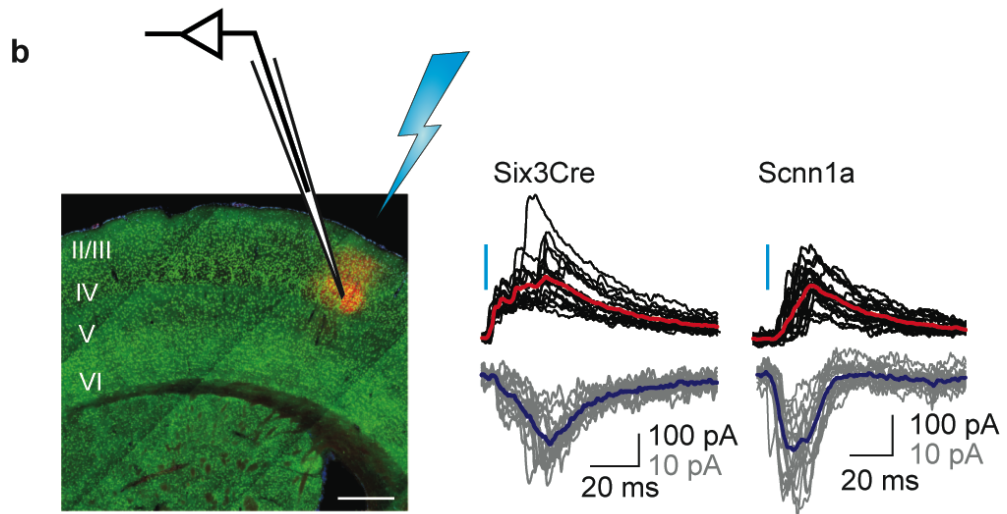
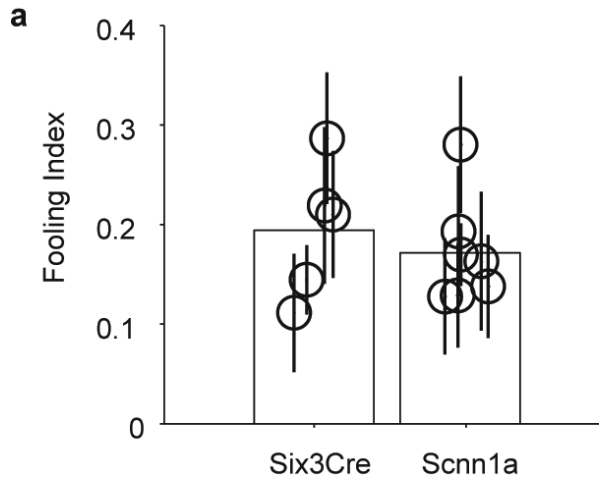


**Figure 9 | Schematic of how L4 spike count codes for object location.**

- Mice report perception of active touch with an object when neural activity occurs during epochs of tactile exploration, and within somatotopic locations matching the moving body part (the C2 whisker). Thus, perceptual reports of touch are gated by sensory expectation.
- Objects at different locations (grey scaled circles) with respect to the whisking region of interest ( $\theta_{ROI}$ ) will produce different numbers of whisker-object contacts and a different pattern of forces/moments, with more numerous contacts and higher average and peak forces/moments for closer (lighter grey) objects.
- Hypothetical distributions of spike count in L4 for trials where the object is in different locations (grey scale, matching panel 'b'). Because of more numerous contacts as well as higher forces/moments, the spike count in L4 will be higher for objects closer to the center of the  $\theta_{ROI}$  (lighter grey).
- The distributions in panel 'c' yield a monotonic spike count code for object location.



**sFigure 10 | Comparison of Scnn1a-Tg3-Cre and Six3Cre mouse lines.**

- a. Fooling Index for the two mouse lines used in this study. We detected no difference between the two lines in illusory touch behavior. Therefore, for all analyses we pooled mice from the two lines. Similarity of behavior is likely due to powerful recruitment of inhibition in both lines, despite expression of ChR2 in GABAergic cells in the Six3Cre but not Scnn1a-Tg3-Cre lines. Error bars, SEM.
- b. Brain slice recordings from barrel cortex L4 neurons of Six3Cre and Scnn1a-Tg3-Cre mice expressing AAV2/5-hSyn1-FLEX-hChR2-tdTomato. Recorded neurons were ChR2-negative but within the ChR2-expressing barrel. EPSCs (grey) and IPSCs (black) were recorded in response to wide-field blue light illumination using whole-cell voltage clamp at -70 mV and 0 mV, respectively, using a cesium-based internal solution. Recordings were conducted at room temperature.
- c. The excitation/inhibition ratio, measured by integrated current (charge transfer), was larger in Scnn1a-Tg3-Cre mice, in which Cre expression does not occur in GABAergic neurons, compared with Six3Cre mice, in which GABAergic neurons do express Cre (one-tailed permutation test). Error bars, SEM.
- d. The inhibition onset latency is longer in Scnn1a-Tg3-Cre mice (one-tailed permutation test). Error bars, SEM.